

Electronic Supporting Information for

Kinetic and mechanistic investigation of the substitution reactions of four and five co-ordinated rhodium stibine complexes with bulky phosphites

Clare Hennion ^a, Klara Jonasson ^b, Ola F. Wendt^{b*} and Andreas Roodt^{a*}

^a *Department of Chemistry, University of the Free State, P.O. Box 339, Bloemfontein, 9300, South Africa. E-mail: roodta@ufs.ac.za; Fax: +27 51 4446384; Tel: +27 51 4012547*

^b *Centre for Analysis and Synthesis, Department of Chemistry, Lund University, P.O. Box 124, S-22100 Lund, Sweden. E-mail: ola.wendt@organic.lu.se*

Contents

1. Figures	S2-S4
2. Tables	S5-S7

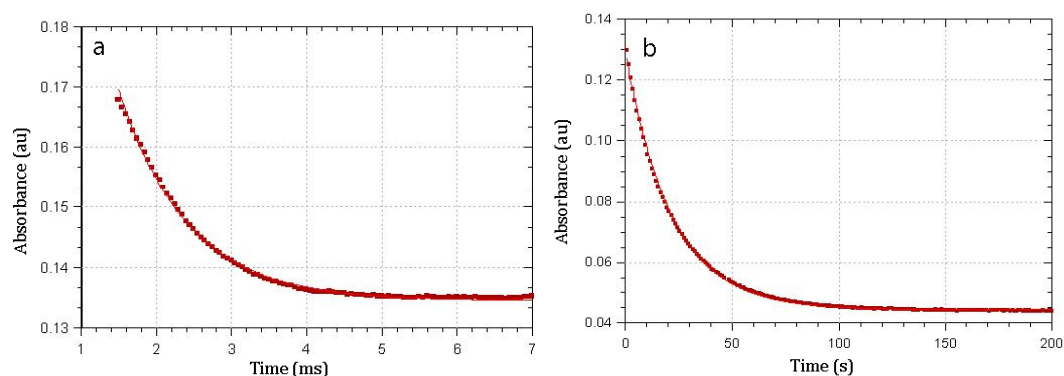


Figure S1. Absorbance change at 310 nm in CH_2Cl_2 at $T = 25^\circ\text{C}$ for (a) the addition of 2,4-TBPP to $\text{trans-}[\text{Rh}(\text{Cl})(\text{CO})(\text{SbPh}_3)_2]$ to form $\text{trans-}[\text{Rh}(\text{Cl})(\text{CO})(\text{SbPh}_3)(2,4\text{-TBPP})]$ and (b) the addition of 2,4-TBPP to $\text{trans-}[\text{Rh}(\text{Cl})(\text{CO})(\text{SbPh}_3)(2,4\text{-TBPP})]$ to form $\text{trans-}[\text{Rh}(\text{Cl})(\text{CO})(2,4\text{-TBPP})_2]$. $[\text{Rh}] = 0.25\text{ mM}$, $[2,4\text{-TBPP}] = 2.5\text{ mM}$. The solid line denotes the best fit to a single exponential.

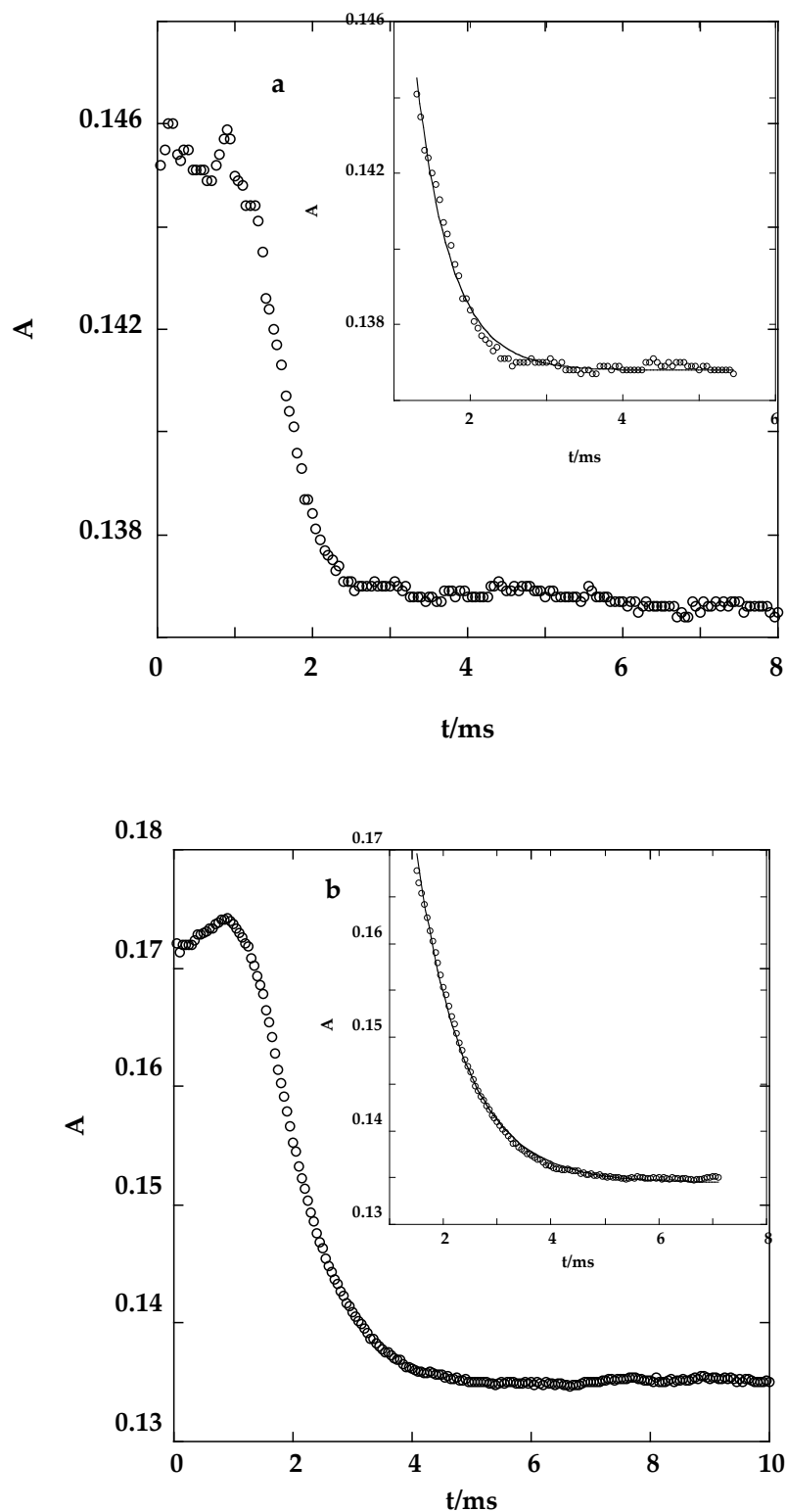


Figure S2. Absorbance change at 310 nm in CH₂Cl₂ at T = 25 °C for the addition of 2,4-TBPP to *trans*-[Rh(Cl)(CO)(SbPh₃)₂] to form *trans*-[Rh(Cl)(CO)(SbPh₃)₂(2,4-TBPP)] [Rh] = 0.25 mM. (a) [2,4-TBPP] = 25 mM. [SbPh₃] = 2 mM. (b) [2,4-TBPP] = 2.5 mM. [SbPh₃] = 10 mM. In the inset the solid line denotes the best fit to a single exponential giving rate constants of 2200±100 s⁻¹ (a) and 1105±12 s⁻¹ (b). The first and last part of the data were cut off.

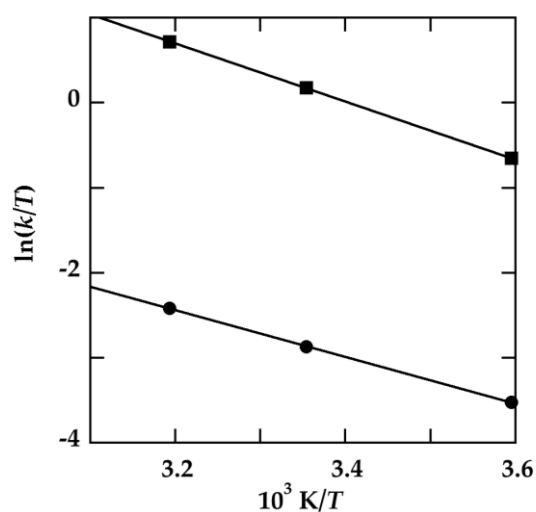


Figure S3. Eyring plot for the direct path in the second reaction in Scheme 1 in different solvents. (●) Dichloromethane, (■) Ethyl acetate. Individual rate constants (in $\text{mol}^{-1} \text{dm}^3 \text{s}^{-1}$) at 278.2, 298.2 and 313.2 K are: 8.22 ± 0.25 , 17.0 ± 0.4 , 27.9 ± 0.4 (dichloromethane); 145 ± 0.8 , 355 ± 10 , 642 ± 10 (ethyl acetate).

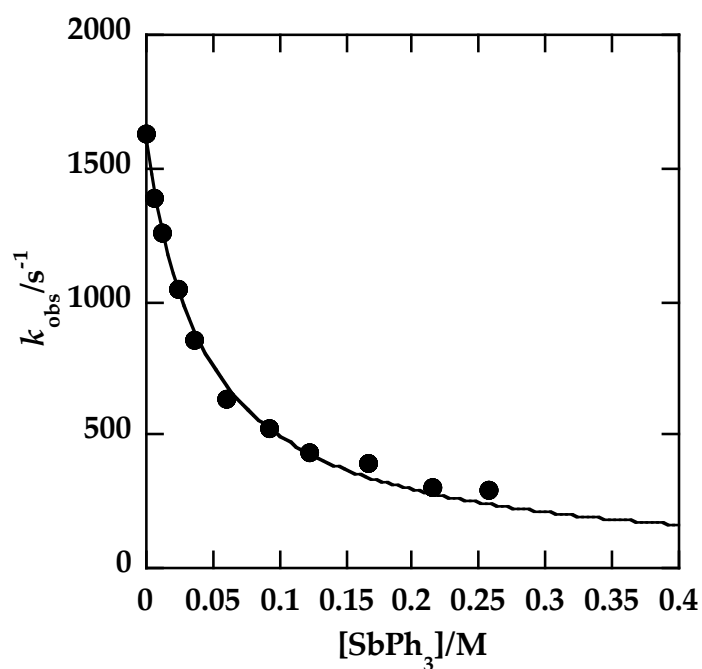


Figure S4. A dissociative pathway for the conversion of **1** to **3** (being four-coordinate) gives rise to a rate law of the form $k_{\text{obs}} = k_1 [2,4\text{-TBPP}] / ((k_{-1}/k_2)[\text{SbPh}_3] + [2,4\text{-TBPP}])$.

The solid line denotes the best fit to this equation with $k_1 = 1605 \pm 25 \text{ s}^{-1}$ and $k_{-1}/k_2 = 0.056 \pm 0.0026$.

Table S1. Observed rate constants at different triphenylstibine concentrations for the reaction of *trans*-[Rh(Cl)(CO)(SbPh₃)₂] (**1**) with 2,4-TBPP in CH₂Cl₂ at 25 °C. [Rh] = 0.25 mM, [2,4-TBPP] = 2.5 mM. Errors are <5%.

k_{obs}/s^{-1}	[SbPh ₃]/mM
1630	0
1390	6.13
1260	12.3
1050	24.5
859	36.8
634	61.3
520	92.0
429	123
389	166
303	215
289	258

Table S2. Observed rate constants at different triphenylstibine concentrations for the reaction of *trans*-[Rh(Cl)(CO)(SbPh₃)₂] (**1**) with 2,4-TBPP in ethyl acetate at -5 °C. [Rh]= 0.25 mM, [2,4-TBPP] = 2.5 mM. Errors are <3%.

k_{obs}/s^{-1}	[SbPh ₃]/mM
973	3.97
780	7.94
598	11.9
527	15.8
439	19.8
425	23.8
255	39.7
139	59.5
100	79.4
150	99.2
116	119

Table S3. Observed rate constants at different 2,4-TBPP concentrations and temperatures for the reaction of $[\text{Rh}(\text{Cl})(\text{CO})(\text{SbPh}_3)(2,4\text{-TBPP})]$ (**3**) with 2,4-TBPP to form *trans*- $[\text{Rh}(\text{Cl})(\text{CO})(2,4\text{-TBPP})_2]$ (**4**) in ethyl acetate. $[\text{Rh}] = 0.25 \text{ mM}$, no SbPh_3 added. Errors are <3%.

[TBPP]/mM	$k_{\text{obs}}/\text{s}^{-1}$ (5 °C)	$k_{\text{obs}}/\text{s}^{-1}$ (25 °C)	$k_{\text{obs}}/\text{s}^{-1}$ (40 °C)
2.50	0.3064	0.7282	1.144
6.30	0.8150	1.832	3.150
12.50	1.701	3.771	6.873
18.80	2.636	5.860	11.03
25.00	3.547	8.533	15.19
37.50	5.355	13.04	23.46

Table S4. Observed rate constants at different 2,4-TBPP concentrations and temperatures for the reaction of $[\text{Rh}(\text{Cl})(\text{CO})(\text{SbPh}_3)(2,4\text{-TBPP})]$ (**3**) with 2,4-TBPP to form *trans*- $[\text{Rh}(\text{Cl})(\text{CO})(2,4\text{-TBPP})_2]$ (**4**) in dichloromethane. $[\text{Rh}] = 0.25 \text{ mM}$, no SbPh_3 added. Errors are <3%.

[TBPP]/mM	$k_{\text{obs}}/\text{s}^{-1}$ (5 °C)	$k_{\text{obs}}/\text{s}^{-1}$ (25 °C)	$k_{\text{obs}}/\text{s}^{-1}$ (40 °C)
2.50	0.02554	0.04581	0.07164
6.30	0.04717	0.07704	0.1665
12.50	0.08377	0.1914	0.3293
18.80	0.1407	0.2880	0.5153
25.00	0.1894	0.3848	0.7135
37.50	0.2955	0.6085	1.018
50.00	0.4129	0.8446	1.400

Determination of Equilibrium Constants.

Thermodynamic determination of the equilibrium constants for the 1st and 2nd step, and the overall equilibrium constant [$K_{tot}=K_1 \times K_2$] (Scheme 2), based on the expressions below were achieved by:

- (i) using the IR Carbonyl $\nu(\text{C}=\text{O})$ data, [Fig. 2, utilising the absorbance after equilibrium at 24h (Ab_{seq})].
- (ii) calculation of the concentrations of different species at equilibrium (denoted by $[..]_{eq}$)
- (iii) approximate deconvolution of the spectra in Fig. 2.

This gave the following equilibrium data, from which the respective equilibrium constants were calculated.

Table S5: Data Calculated from Figs. 1 and 2 in manuscript

Complex	$\nu(\text{C}=\text{O})$	Ab_{seq} Fig 2 at 24h	Molar extinction coefficient, ϵ , from Fig 1	$[\text{Rh}]_{eq}$ (1, 3 or 4)	$[\text{2,4-TBPP}]_{eq}$	$[\text{SbPh}_3]_{eq}$
	(cm^{-1})		($\text{M}^{-1}\text{cm}^{-1}$)	(M)	(M)	(M)
1	1969	0.076	64	0.0012	0.00055	0.0046
3	1994	0.115	58	0.0020	--	--
4	2009	0.095	74	0.0013	--	--

Expressions for calculation of Equilibrium constants (Based on Scheme 2) ^(a)	Constant	Value ^(b)
$K_1 = [\text{3}] / ([\text{1}] * [\text{2,4-TBPP}])$	$K_1 (\text{M}^{-1})$	$(3.0 \pm 0.9) \times 10^3$
$K_2 = ([\text{4}] * [\text{SbPh}_3]^2) / ([\text{3}] * [\text{2,4-TBPP}])$	$K_2 (\text{M})$	$(2.5 \pm 0.7) \times 10^{-2}$
$K_{tot} = ([\text{4}] * [\text{SbPh}_3]^2) / ([\text{1}] * [\text{2,4-TBPP}]^2)$	$K_{tot} = (K_1 \cdot K_2)$	$(7.5 \pm 3.2) \times 10$

(a) *trans*-[Rh(Cl)(CO)(SbPh₃)₂] (1); *trans*-[Rh(Cl)(CO)(SbPh₃)₂(2,4-TBPP)] (3); *trans*-[Rh(Cl)(CO)(2,4-TBPP)₂] (4)

(b) due to uncertainty associated with the deconvolution, esd's of ca. 30% are estimated.